Periodicals of Engineering and Natural Sciences ISSN 2303-4521
Vol. 9, No. 2, April 2021, pp.762-773

Highly sensitive fiber-optic temperature sensor based on tapered no-core fiber for biomedical and biomechanical applications

Mohammad M. Hasan[1], Hanan J. Taher[2], and Saif A. Mohammed[3]
[1,2,3]Institute of laser for postgraduate studies, Baghdad University, Baghdad, Iraq

ABSTRACT

A low-cost, easy to fabricate real-time temperature sensation device built on an In-Line Mach–Zehnder interferometer basis was manufactured by fusing a segment of no-core fiber amongst two fibers of single-mode. Two different structures, tapered no-core fiber, and untapered no-core fiber both retaining acrylate polymer coating were investigated. The 3 cm length tapered no-core fiber sensor showed the highest sensitivities of ~ -1.943 nm $\circ C^{-1}$ and ~ -1.954 nm $\circ C^{-1}$ for two different dips respectively. The sensor exhibited high linearity with a very good resolution of 0.0102 ◦C. making the most of the high coefficient of thermal expansion, thermo-optic properties of the acrylate polymer, and the tapering effect, the sensor could be utilized in many temperatures observing applications like biochemical labs, biomechanical studies, and bio-sensing analyses.

Keywords: sensor; no-core fiber; Mach-Zehnder; interferometer; temperature

Corresponding Author:

Mohammad M. Hasan
Institute of laser for postgraduate studies
Baghdad University
Baghdad. Iraq
mohammad.muzahim@gmail.com

1. Introduction

All-fiber sensors have been increasingly investigated for the last fifteen years, they have drawn significant attention from researchers because of their superior features to electronic sensors such as operating in a harsh environment, prompt response to changes, immunity to electromagnetic interference, high resolution, bio-compatibility, and compactness [1]. A great number of fiber sensor structures were developed to measure diverse types of physical measurands such as temperature [2], strain [3], relative humidity [4], pH number[5], stress[6], and so on. Temperature is an influential physical parameter that needs to be monitored in many engineering applications, biomedicine labs, and biomechanical researches. Temperature sensors were consistently developing for the past decade a huge amount of researches were conducted and different structures were developed based on intensity modulation [7], wavelength modulation [8], and polarization modulation [9] Furthermore, wavelength modulated sensors have shown proven results and steady performance [10]. The operation principle of wavelength modulated temperature sensors can be explained by studying the influence of imposing the fiber sensor on temperature variations and observing the shift in the Interference dips or peaks. Moreover, sensitivity enhancement can be achieved with the proper design of these sensors. Mach-Zehnder interferometric sensors (MZI) have widely been employed in creating thermometric optical fiber sensors, on account of this, the MZI has become the basis of immeasurable counts of optical fiber temperature sensors[11,12].MZI temperature sensors were technologically advanced and various setups were developed exhibiting interesting outcomes in terms of sensitivity, however high cost, long fabrication time, fragility, difficulties of handling after fabrication and the alteration of results due to simple movement have restricted these sensors to be deployed in real measurement systems. Single-mode-no-core fiber-single-mode (SNS) fiber structure has been reported in quite a few publications and has been showing some interesting results [13-15]. The SNS structure is a variant of single mode-multimode-single-mode (SMS) structures with enhanced sensitivity to the changes of the surrounding as it has no core, the glass waveguide can be in direct contact with the environment, consequently, there is no need to etch the cladding to enhance the sensitivity such as those of typical multi-mode fiber MMF. Heat sensitive coating can be applied to the no-core fiber sensing head for temperature sensitivity enhancement. No-core fiber (NCF) has many other advantages, on top of these

advantages is relatively low cost as compared to other special type fibers such as photonic crystal fibers(PCF). Polymer coatings have been reported to greatly enhancing thermal sensitivities as high as many orders in magnitude in some fiber-optic temperature sensors. Polymers have a high thermal expansion coefficient (TEC), mechanical toughness, non-toxicity, ease of handling, and cheapness [16-18]. Proper length selection for the active sensing element is the key success of designing MZI based optical fiber temperature sensors as well as a good understanding of the transmission spectrum characteristics. In this work, we have employed two sensitivity improving techniques at the same time by keeping the original polymer coating and inducing tapers for further sensitivity improvement. Two different structures, tapered single-mode-no-core fiber-single-mode polymer-coated (TSNS-PC) and untapered single-mode-no-core fiber-single mode polymer-coated (SNS-PC) both retaining their factory-made polymer coating of the no-core fiber sensing element, each at three different lengths was fabricated. The transmission spectrum of each sensor 2cm, 3cm, and 4 cm no-core fiber element has investigated a total of six different structures, the 3 cm TSNS-PC transmission has shown two well-separated interference dips which were followed up, the sensor was subjected to temperature range (30–45) ◦C the obtained sensitivities were as high as ∼ −1.943 nm ◦C−1 and ∼ −1.954 nm ◦C−1 for two different dips, respectively. The sensor exhibited high linearity of the spectral shift against temperature variance. The experimental outcomes revealed that the sensitivity was greatly improved by tapering affect ∼53%. The increasing temperature sensitivity is mostly ascribed to the high coefficient of thermal expansion, thermo-optic properties of the acrylate polymer coating, and the tapering effect that promotes more evanescent wave penetration to the outer medium. The investigation also included a parallel procedure of studying the behavior of the optical intensity feedback for observing the intensity responses in both tapered and untapered sensors.

2. Working principle and theoretical analysis

A schematic diagram of the built TSNS-PC thermometric sensor is illustrated in Figure1. The TSNS-PC fiber structure is created by fusing a part of NCF amongst dual fibers of a standard single-mode. As the fundamental core mode advances from lead-in single-mode fiber (SMF) and reaches the first tapered region, higher-order modes are excited these modes will advance in the NCF suffering many reflections then re-couple in the second taper to continue the propagation to the lead-out SMF constituting an interferometric pattern based on MZI. Since the taper can be attained via a fusion splicer, the formed taper shape can flexibly be designed by adjusting arc-current, arc- time, or arc-power leading to different coupling constants from the lead-in SMF to the NCF section, consequently, an adjustable design of the sensor structure [19]. In this work, the TSNS-PC fiber construction is a typical SMS design where the no-core fiber (NCF) lays amongst two single-mode fibers (SMFs) that are aligned optically, the NCF segment and its protective polymer coating signify the multimodal waveguide core and the correlated cladding, respectively. The easiest way to examine the principles of MMI impacts in fiber-optics can be maintained by fusion splicing an SMF straightly with a step-indexed type MMF. As light-wave is conjoined into the MMF, the input domain could be disintegrated into guided modes backed by the multimode fiber, consequently, an interference phenomenon between them takes place. It is well accepted that when light propagates in single-mode-multi-mode-single-mode (SMS) interference peaks or interference dips in the transmission spectrum is created at optimized lengths for a given multimode fiber as they advance, assembling mimics of the input domain at identified spaces all over the length of the MMF [20].

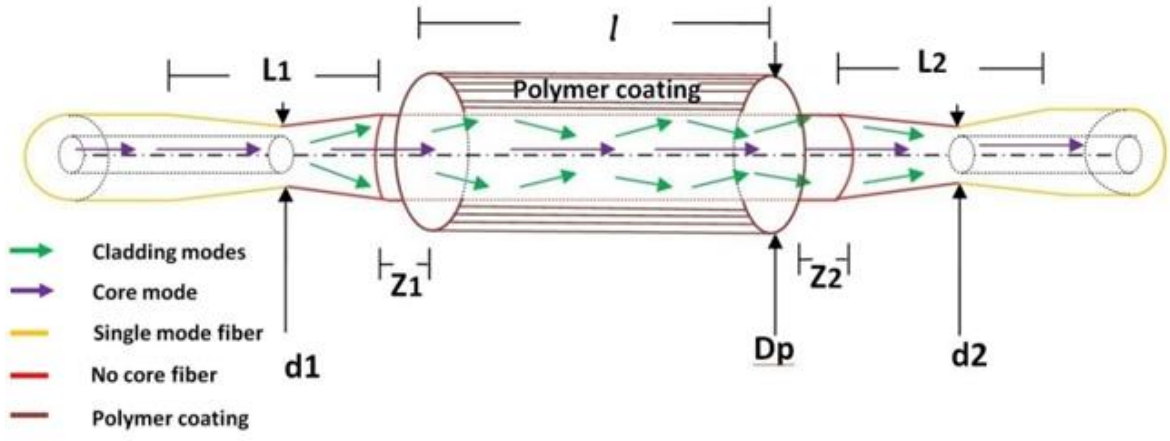

Figure. 1. Schematic diagram of the tapered no core fiber temperature sensor

The proportionate spectral shift induced by temperature variance can be given as [21]

$$\frac{\Delta\lambda a}{\lambda} = (\alpha a+\xi a)\,\Delta T\,, \qquad (1)$$

Where αa and ξa are, respectively, thermal expansion coefficient (TEC) and thermos-optic coefficient (TOC) of the NCF material. If the polymer coating was stripped-off, according to the equation above temperature rise would allow the interference dip location to move linearly to longer wavelengths. (red-shift) and the thermal sensitivity would purely be dependent on the specification of the NCF glass material. The TSNS-PC fiber configuration, however, is also sensitive to the index of refraction variation of the protective acrylate coating which acts as cladding in our case. Assuming the TOC of the acrylate polymer coating is ξb, the spectral shift introduced by the acrylate polymer coating index variations due to temperature rise can be addressed as [22].

$$\frac{\Delta\lambda b}{\lambda} = \rho\xi b\Delta T\,, \qquad (2)$$

Where ρ is perpetual. When ξb is largely negative, the impact of the thermo-optic response of the protective polymer coating presents a negative sensation rate of temperature to the sensor. As the sensor is not strained the proportionate total wavelength shifting induced by the variation of temperature would be as in [22,23]

$$\Delta\lambda = \Delta\lambda a + \Delta\lambda b = [(\alpha a+\xi a) + (\rho\xi b)]\,\Delta T \qquad (3)$$

The theoretical calculation of Eq. (3) can predict that the wavelength shift is dependent on both NFC glass and the polymer coating, accordingly, the thermal sensitivity of the sensor is affected by the thermal properties of the NFC material and the polymer coating. For silica fibers, $\alpha a \sim = 5.5 \times 10^{-7}\ K^{-1}$ and $\xi a \sim = 6.9 \times 10^{-6}/°C$. A factory-made protective polymer coating (UV-curable acrylate) with a large negative TOC ~ -4×10^{-4} retained in the fabrication of the temperature sensor, as (ρξb) term is a large negative value, (blue-shift) is expected [24,25].

3. Temperature sensor design and fabrication

3.1 Tapered temperature sensor fabrication

In the fabrication process of the temperature sensor, a segment of NCF (FG125LA by Thorlabs) with 125 μm glass diameter retaining its acrylate polymer coating of 62.5 μm thickness cleaved and spliced between two

Table 1. Fusion splicing parameters for the tapered regions

Fiber Type	Proof test	Fiber angle limit	Gap(μm)	Arc current (bit)	Rearc time(ms)	Offset(dB)
MM-SM	on	1.0◦	18	125 ~ 15.6 mA	1000	0.00

(Corning SMF-28) pigtails .to make the splicing applicable ~2 mm of the polymer coating stripped off from both ends of the NCF, the Lead-in SMF connected to a broad-band light source (SLD1550S-A1, by Thorlabs) with a spectral range of 1450–1650 nm and the Lead-out SMF attached to an 0.02 nm resolution optical spectrum analyzer (Yokogawa AQ6370).To obtain the tapering, a set of parameters were configured using a fusion splicer (SWIFT KF4, America Ilsintech) the fusion splicing parameters are listed in Table1. The taper lengths and waist diameters are L1, L2, d1, and d2 and their dimensions are 462.592 μm, 464.884 μm, 90.782 μm, 86.269 μm,

respectively. The retained polymer protective coating length is labeled *l* in Figure 1. And is ~ 2.96 cm while Z1=Z2 =~ 2 mm stripped of polymer from both sides of the NCF to enable fusion splicing with the single-mode fibers. Infrared light will propagate from the broadband source to the active sensing head (i.e. polymer-coated no-core fiber) eventually to the OSA for investigating the transmission spectrum of the sensor. In our work, two different structures were tested. First, using automatic fusion splicing parameters to fuse the polymer-coated NCF active sensing segment (i.e. no tapering induced), then using a set of predefined parameters to form tapering at both splicing joints. The sensor's experimental setup is illustrated in Figure 2.

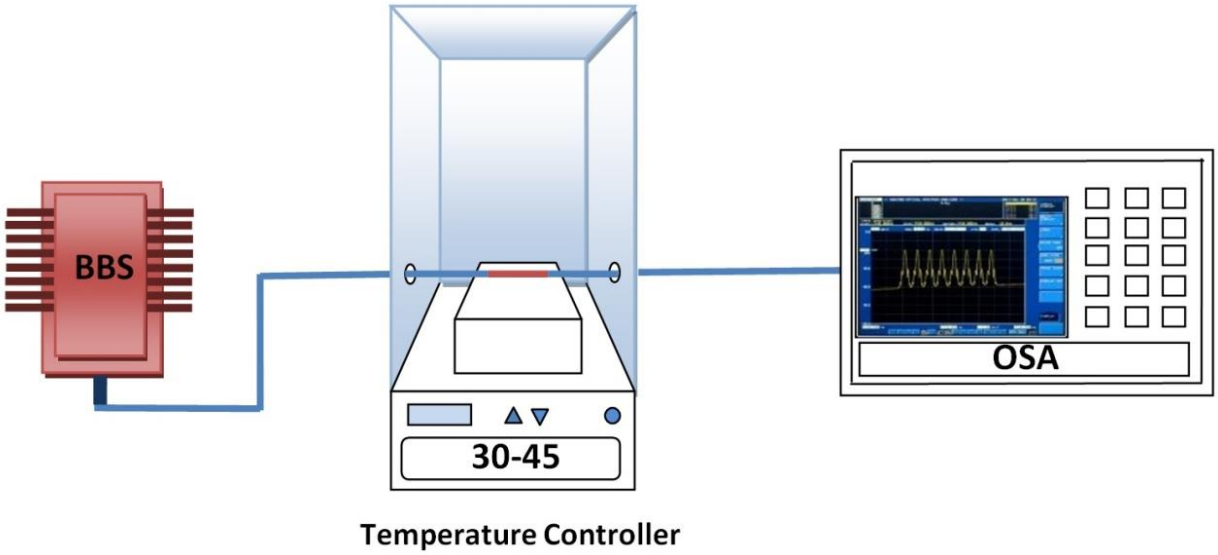

Figure 2. Experimental setup

3.2 Length selection characterization

In pursuance of the optimal length selection for the temperature sensor, the spectra of transmission for the three varying NCF lengths investigated 2 cm, 3 cm, and 4 cm with and without the tapered splicing joints, as illustrated in Figure 4. It can be seen that for 2 cm length, resonance dips are virtually imperceptible with a relatively small extinction ratio, which might contribute to less signal coupling into higher-order modes and more optical power in the fundamental mode. As the length is increased to 4 cm, more than two interference dips were observed with good extinction ratios, however, the dips were either overlapping or adjacent, forming interference patterns that are obvious but undistinguishable this might be introduced because of a significant optical power loss due to the variance in optical path lengths of different modes along the NCF length. Furthermore, at 3 cm length, one interference dip was observed in the untapered SNS-PC with a reasonable extinction ratio of 16.3 dB, while two dips were observed in the TSNS-PC at an extinction ratio of 23.8 dB for the first dip. For the second dip, the extinction ratio was around 12.5 dB both dips were followed up in the investigation process for sensitivity comparison. Thus, with a 3 cm length, the most advantageous interference minima can be attained as well as good extinction ratios. The spectral span between the dips for the untapered sensor was good as well in the tapered sensor. The tapering length and waist diameter were decided after a trial-and-error procedure, reduced taper waist below 80 µm denoted to more optical intensity degradation in the transmission spectrum and higher power loss, accordingly, the tapering parameters were fixed for the best tapering waist and length as mentioned in the previous paragraph. The tapering was also examined via an optical microscope for confirming the homogeneity and non-existence of any distortion on the splicing joints which might greatly affect the coupling efficiency and alter the results Figure 3. Illustrates the microscopic images for both tapers. The selected length is also advantageous as it is easily fabricated and can be refabricated in few minutes in case of fracture unlike complicated structures that are both costly and time-consuming. The transmission spectrum of both SNS-PC and TSNS-PC was examined at room temperature 20 °C before experimenting with different NCF length and are illustrated in Figure 4.

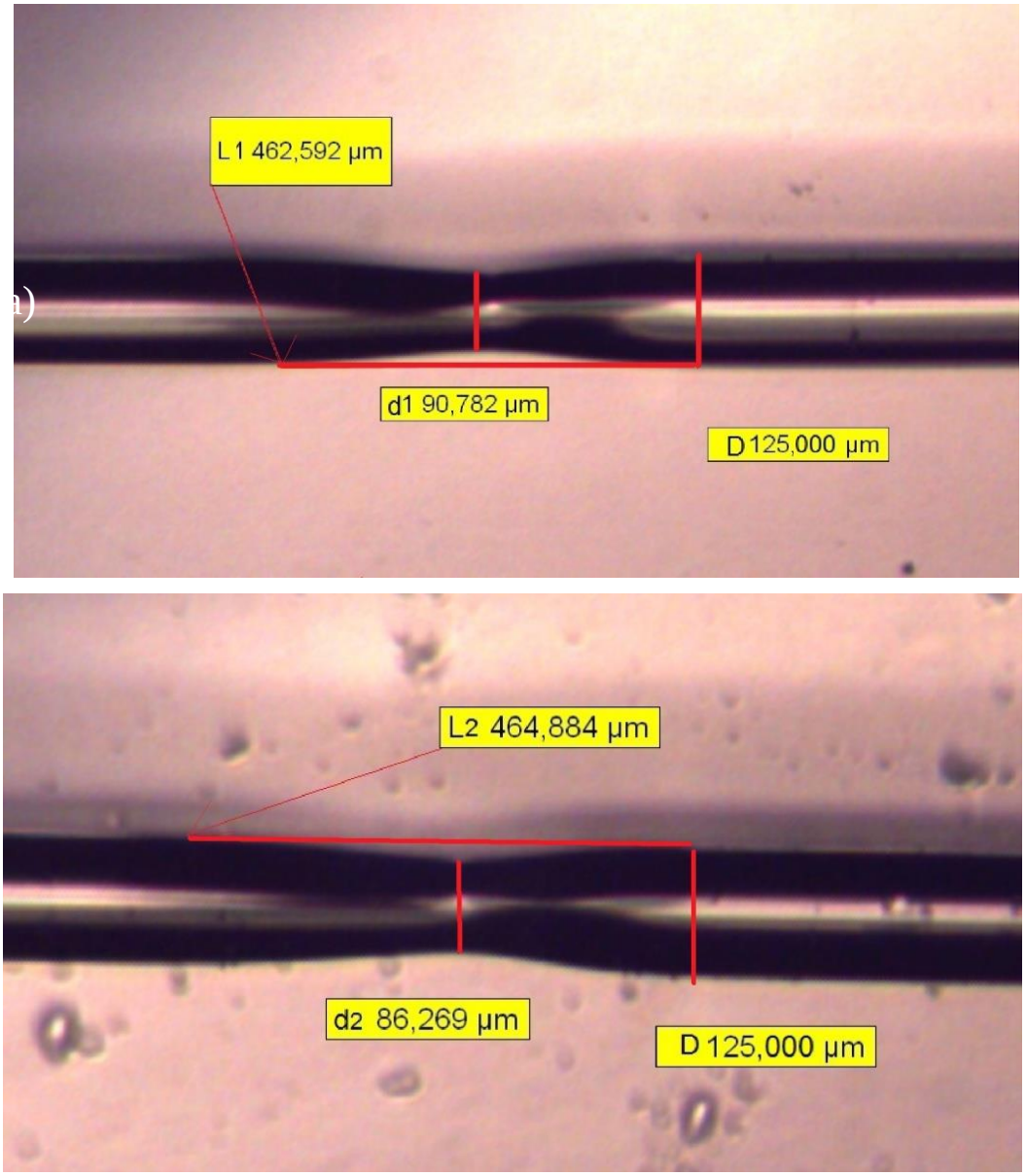

Figure. 3. Microscopic images of the tapered joints 40 X (a) first taper (b) second taper

4. Results and discussion

To examine the sensitivity of temperature for the TSNS-PC structure, the sensor was situated in direct touch to the outward area of a hot-plate without applying any tension to avoid strain. Then gradually rising the temperature starting from 30 ◦C to 45 ◦C step of 3 ◦C using an adjustable heat controller all covered by a sealed glass chamber, the selected temperature range is within several biomechanical and biomedical applications. First, the un-tapered SNS-PC sensor was made-up by fusing a section of NCF without stripping off the polymer coating. The transmission spectrum of the un-tapered 3 cm NCF sensing head revealed an interference minimum at 1574.5 nm with around 16.3 dB extinction ratio. The spectral response of the un-tapered SNS-PC sensor is illustrated in Figure 5. The dip exhibits a shift toward shorter wavelengths with increasing temperature and exhibits a shift towards longer wavelengths with decreasing temperature, at the same time the optical intensity values decreased then increased with heating and cooling, sequentially. The wavelength response and the intensity response of untapered SNS-PC with rising and decreasing temperatures are given in Figure 6. Out of the obtained outcomes, the linear fitting graph of the spectral blue-shift and intensity profile

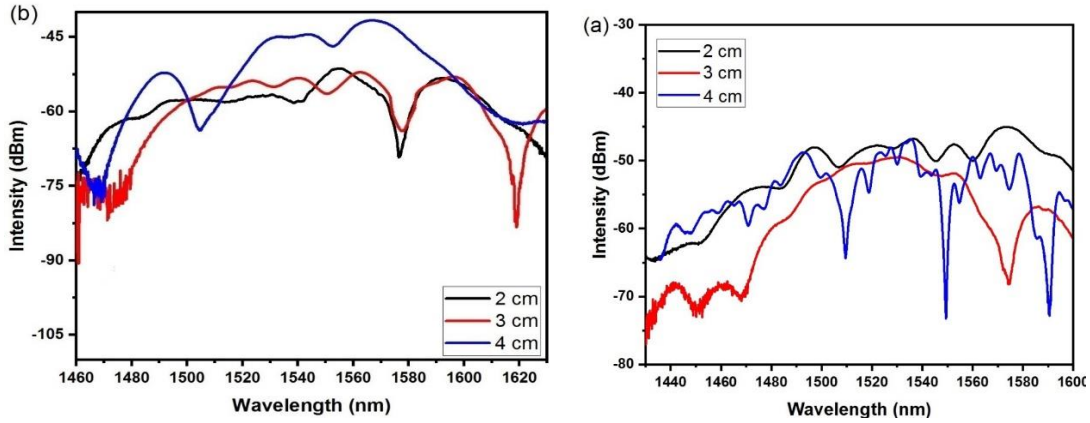

Figure 4. Spectra of transmission of the SNS-PC sensor at varying lengths: (a) without tapering, (b) with tapering

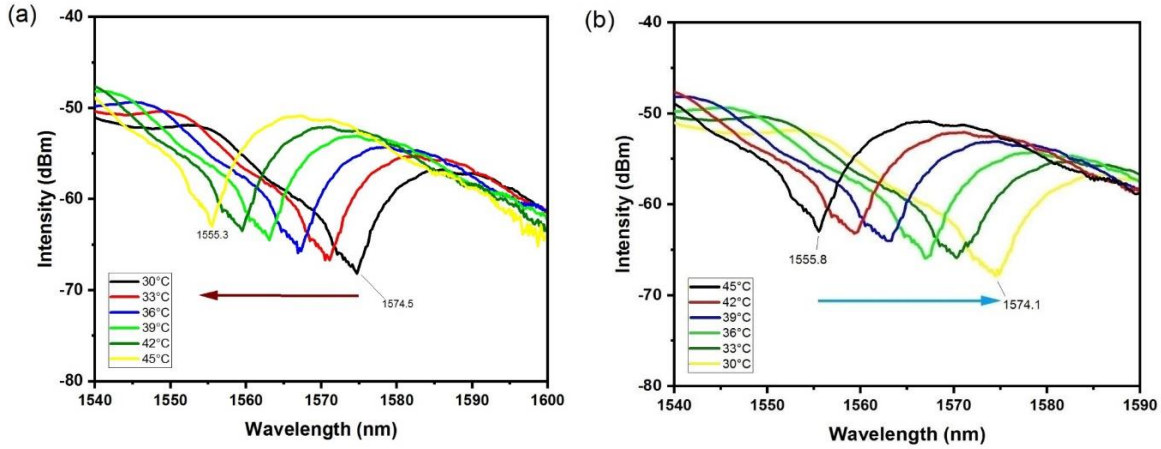

Figure 5. Spectral response of the untapered SNS-PC sensor, as the temperature varied (a) 30-45 ◦C (b) 45 - 30 ◦C

Both come out with a very good coefficient of linear regression, the values of R^2 for the spectral blue-shift and the corresponding intensity feedback were around 0.9985 and 0.9277, sequentially. The calculated spectral sensitivity and intensity slopes were −1.2628 nm/ ◦C and 0.3178 dB/ ◦C, sequentially. The total wavelength shift induced by heating was around 19.2 nm. As indicated in the below graph the wavelength shift induced by heating is heading towards a shorter wavelength and the intensity also linearly decreases in the untapered SNS-PC, the cooling cycle nearly exhibited an opposite behavior to the heating cycle which confirmed the steady behavior of the sensor in response to thermal effect. Then, a second active sensing head examined the TSNS-PC of 3 cm length NCF with both splicing joints tapered as per the given parameters of Table 1.

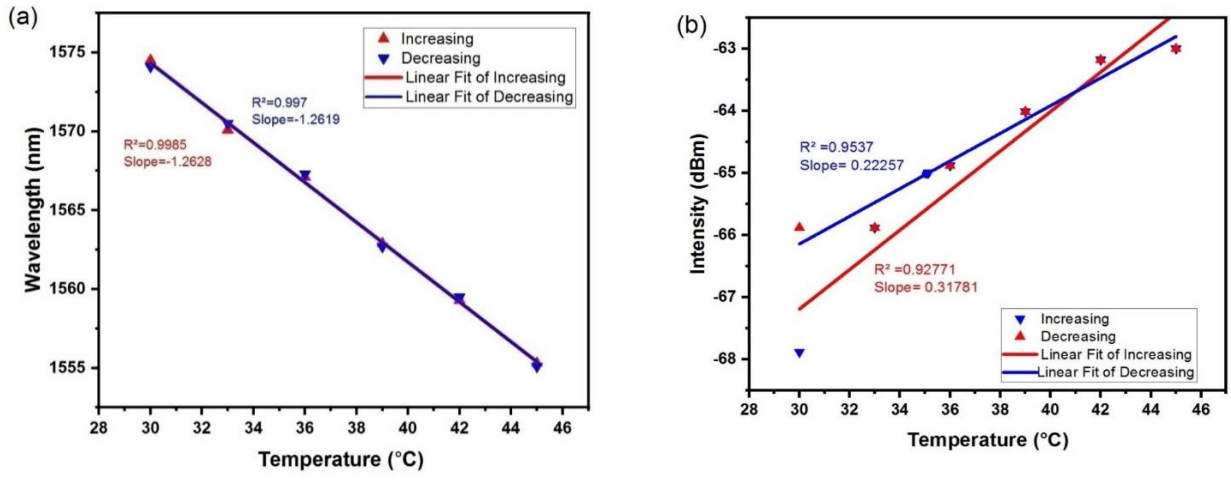

Figure 6. Interference dip behavior with temperature variation against (a) wavelength (b) optical intensity of the sensor

The tapering effect can enhance the sensitivity by permitting more evanescent waves to couple with the surrounding medium and reducing the number of higher-order modes contribution in the coupling, consequently, the more optical power in the LP01 and LP11. From the spectral response of Figure7.the tapered single-mode-no-core fiber-single-mode showed two interference dips at 1618.9 nm and 1577.7, respectively. First dip revealed a very good extinction ratio of around 23.8 dB this dip wavelength exhibited an excellent blue-shift of nearly 29.2 nm. However, the optical intensities of the output wavelengths experienced an increase then a consistent decrease along with temperature rising from 30 ◦C to 45 ◦C step 3 ◦C. The determining sensitivity of the TSNS-PC is illustrated in Figure 8a. for dip 1 it revealed a spectral sensitivity of around −1.9438 nanometer per single degree centigrade, however, the optical intensity revealed a polynomial behavior. The linear fitting coefficient was 0.9969 for the wavelength feedback while the polynomial regression coefficient was 0.9164 for the optical intensity feedback Figure 8b.

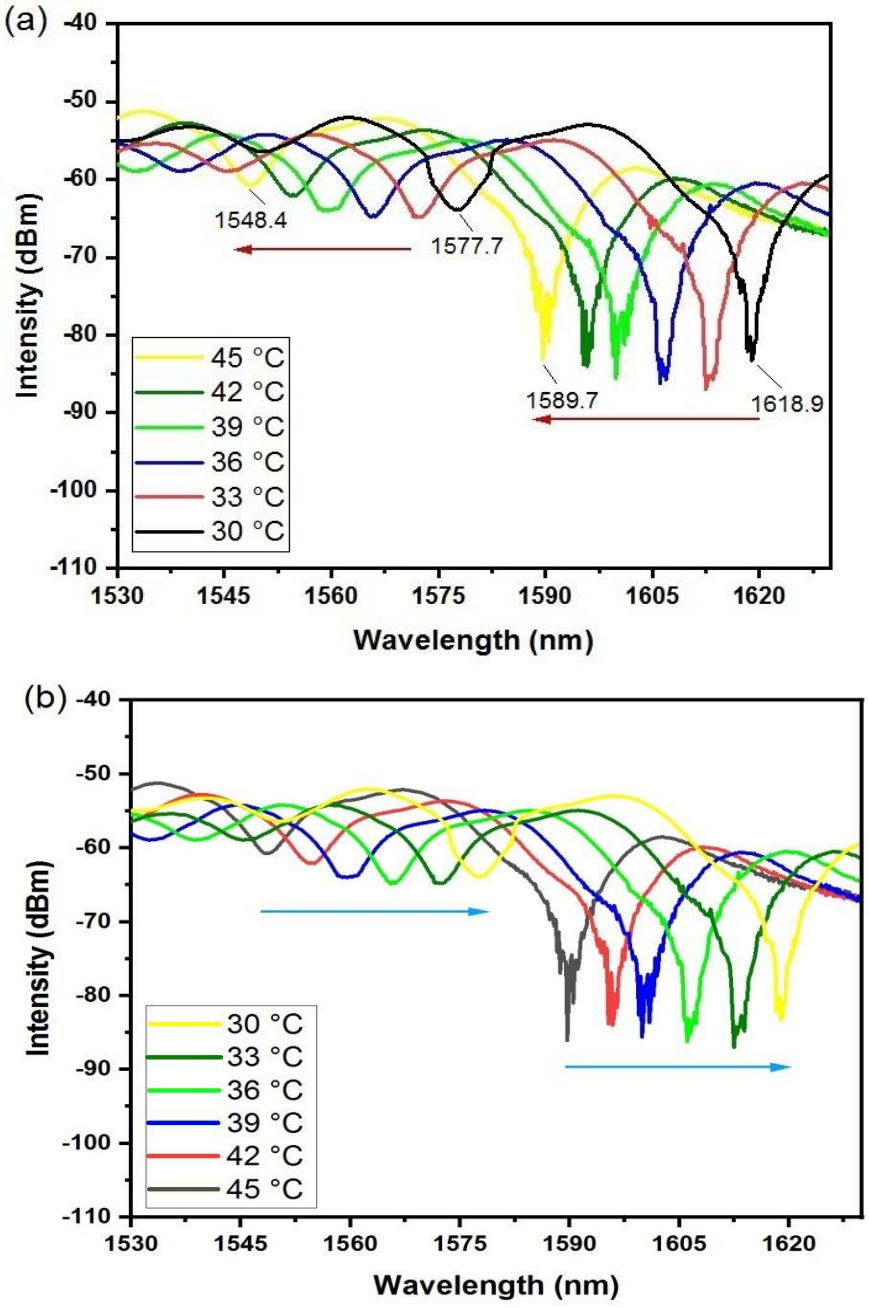

Figure 7. Spectral response of the dip1 tapered TSNS-PC sensor, as the temperature varied (a) 30 - 45 ◦C and (b) 45 - 30 ◦C

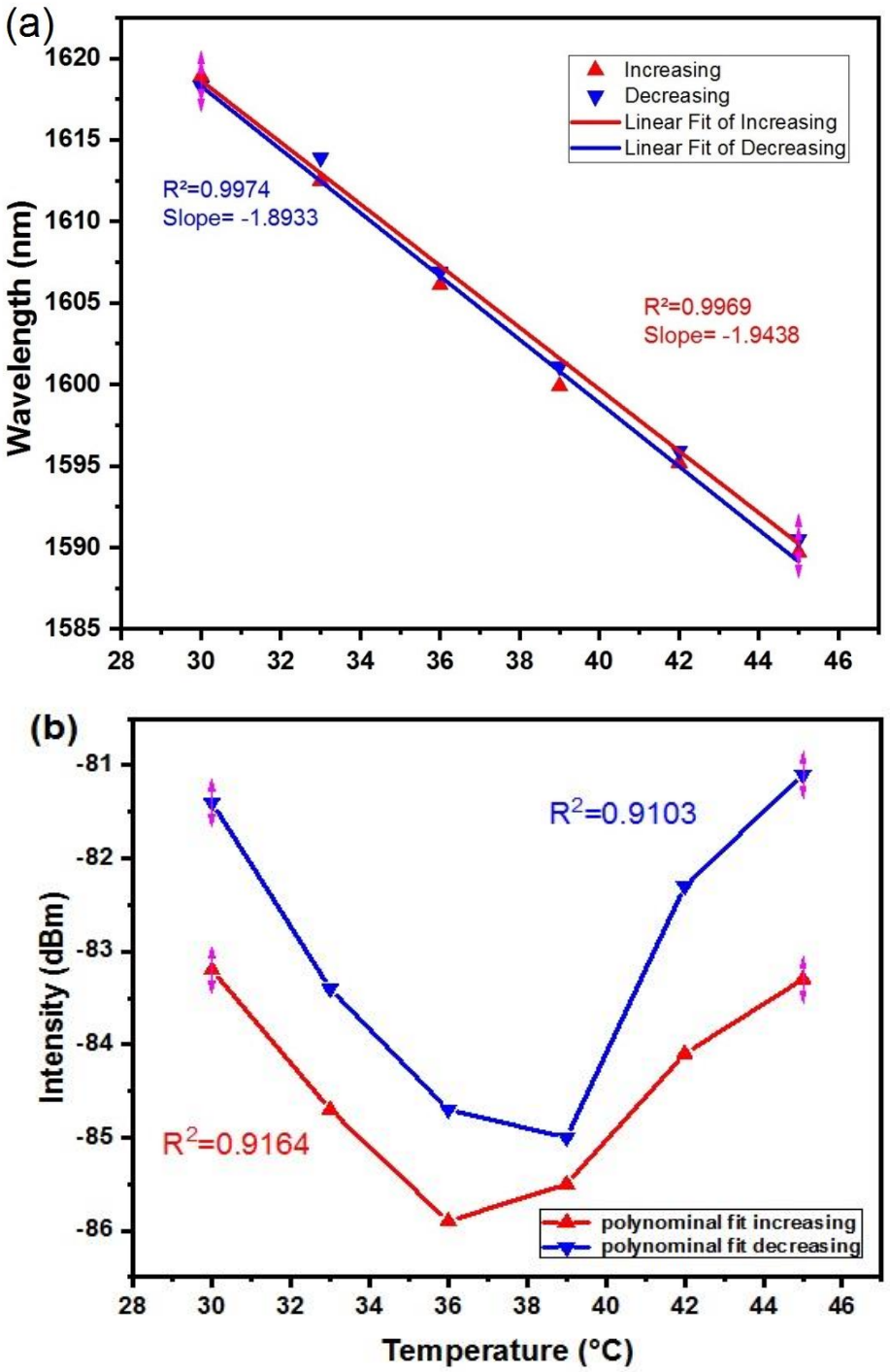

Figure 8. dip1 behavior with temperature variation against (a) wavelength (b) optical intensity for tapered sensor

The obtained results indicated that the wavelength behavior remained linear with temperature variance while the intensity behaviors in the TSNS-PC exhibited nonlinear feedback. To compare the spectral shift behavior and the sensitivity behavior, dip2 of the TSNS-PC examined as well, it showed 12.5 dB extinction ratio at 1577.7 nm, the spectral shift of the second dip is illustrated in Figure 7. The second dip exhibited 29.3 nm shift toward shorter wavelengths as well. The calculated sensitivity of the second dip, the TSNS-PC of 3 cm NCF sensing head for both spectral responses with temperature variance is given in Figure 9a

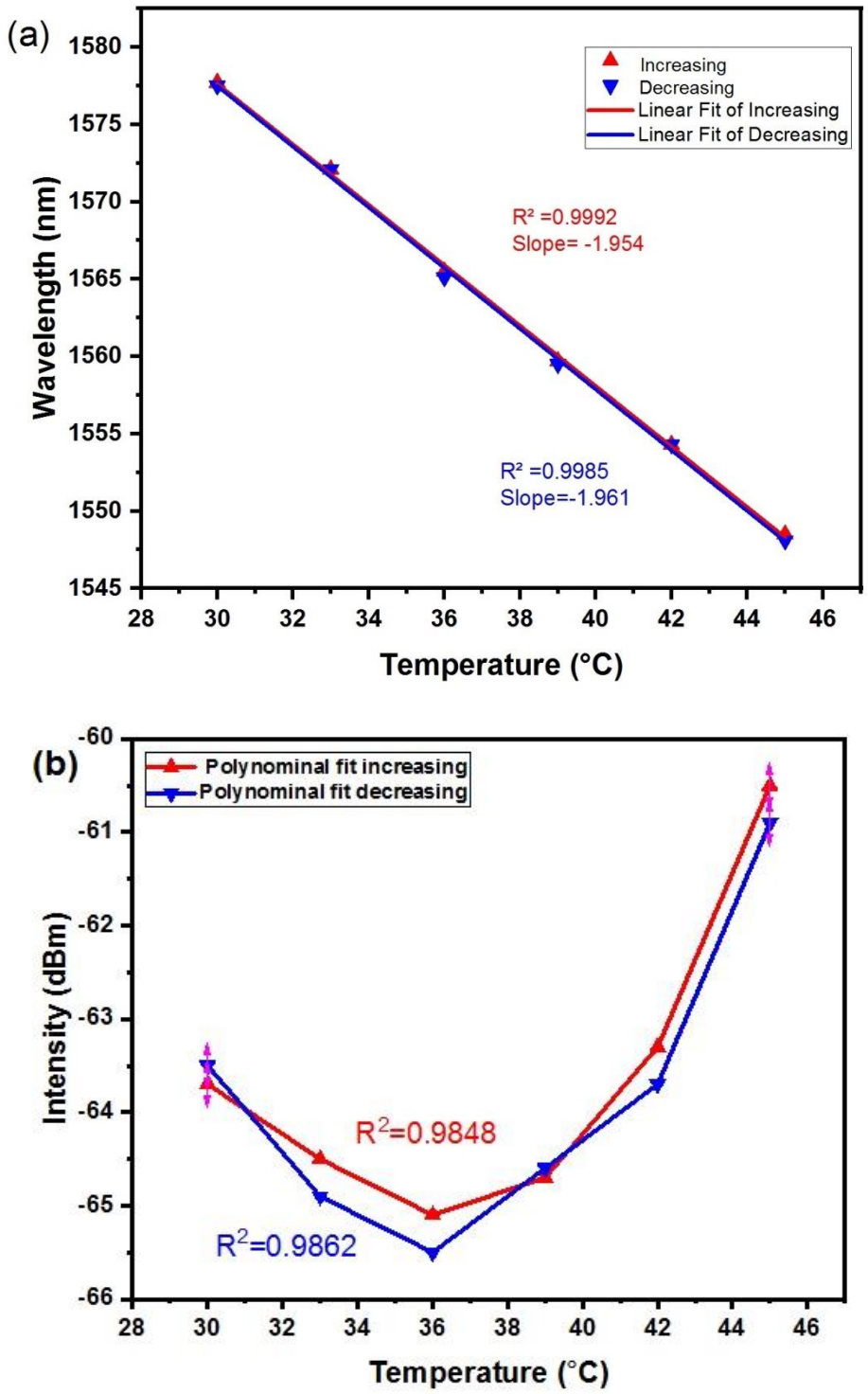

Figure 9. Dip 2 behavior with temperature variation against (a) wavelength (b) intensity for the tapered sensor

It showed a spectral sensitivity of around −1.954 nm/ ◦C. The second interference dip's calculated coefficient of linear regression is 0.9992 for the spectral response while the intensity response followed a polynomial behavior, the determined polynomial coefficient of regression was around 0.9848 as illustrated in Figure 9b. From the maintained results of dip2, the behavior of both wavelength response and intensity feedback remained consistent as those of dip1, they revealed a linear response to the spectral shift and nonlinear feedback for the optical intensity with thermal variance. The tapered sensor exhibited similar behavior with a previously published improved tapered temperature sensor with an approximately similar TOC coating [26]. The shift towards shorter wavelengths of the fabricated sensor could probably be associated with the bigger index of refraction of the polymer coating material, along with the refractive index of NCF being reduced because of the large negative TOC, of the protective coating which is about – 4 x 10^{-4} / ◦C [16, 27]. The resolution calculation

was estimated by dividing the spectrum analyzer resolution by the obtained sensitivity of the tapered sensor which was around 0.0102 ◦C. It can be seen from the experimental results the tapering effect significantly improves the sensitivity about 53% in the TSNS-PC temperature sensor by allowing more evanescent waves coupling into the surrounding medium, for the TSNS-PC setup, there are powerful modal interferences at the tapered no-core fiber-optic segment. That is due to the strong concentration of infrared light at the Lead-in taper transient part. plus, the filtering effect which reduced the higher-order mode propagation, plus in the tapered sensor mode counts that are along the Lead-out taper transient section are fewer than those of the un-tapered SNS-PC fiber structure, consequently, a significantly enhanced sensitivity [28-33]. The effectiveness of our proposed all-fiber thermometric sensor is listed in contrast to some lately stated temperature sensors centered on various MZI setups. The sensitivities, temperature ranges, and linearity coefficients are recorded in Table 2. Our suggested sensor is outstanding for sensitivity as matched to the earlier published sensors. Considering the proposed sensor's dominance in terms of max sensitivity, compactness, cost-effectiveness, and ease of manufacturing, it could largely be used in a wide variability of biomechanical applications, biomedical and industrial applications.

Table 2. Performance comparison with different sensors of temperature

Fiber sensor setup	Temperature range °C	Sensitivity pm C^{-1}	R^2	Ref.
Half-tapered SMS fiber structure	25-50	72	>0.99	29
Symmetrical Double-Grooved Structure	20-90	230	0.99	30
Mach-Zehnder fiber sensor based on thin-core fiber	25-80	65	0.996	31
Folded-tapered multimode-no-core fiber sensor	20-90	59.8 ,64.8	0.99	20
Tapered SNS-PC	30-45	-1943, -1.954	0.996	our work

5. Conclusion

Finally, we demonstrated the use of a single-mode no-core fiber-single mode tapered interferometric sensor for temperature sensing purposes in an experimental environment. A novel high sensitivity thermometric all-fiber sensor built on basis of Mach-Zehnder retaining factory-made polymer coating is investigated both with and without tapering effect. An impressive method for further enhancement can be adapted by stripping the polymer jacket and applying various heat-sensitive coating layers to the no-core fiber sensing element, which might increase the sensing capability by several orders of magnitude. Our proposed all-fiber temperature sensor outperforms previously recorded fiber temperature sensors in terms of thermal sensitivity ~ −1.943 nm ◦C^{-1}., resolution 0.0102 ◦C, ease of fabrication, and high linearity with wavelength shift. The proposed thermometric sensor is suitable for temperature monitoring in the areas of biochemistry, biomechanics, and biomedicine.

Disclosures no conflicts of interest declared by authors

Acknowledgement This research was supported by the higher education and scientific research ministry of Iraq and Baghdad University (UoB).

References

[1] P. Roriz, S. Silva, O. Frazão, and S. Novais, “Optical Fiber Temperature Sensors and Their Biomedical Applications,” *Sensors*, vol. 20, no. 7, p. 2113, Apr. 2020.

[2] G. Zhou et al., “A Low-Cost High-Temperature Sensor Based on Long-Period Fiber/Microfiber Gratings by Local Fictive Temperature Modification,” Journal of Chemistry, vol. 2020, pp. 1–6, Jun. 2020.

[3] L. Dong, T. Gang, C. Bian, R. Tong, J. Wang, and M. Hu, "A high sensitivity optical fiber strain sensor based on hollow core tapering," Optical Fiber Technology, vol. 56, p. 102179, May 2020.
[4] H. Alsweefe, S. K. Al-Hayali, and A. Al-Janabi, "Efficient humidity sensor based on an etched no-core fiber coated with copper oxide nanoparticles," J. Nanophoton., vol. 12, no. 04, p. 1, Dec. 2018.
[5] X. Cheng, J. Bonefacino, B. O. Guan, and H. Y. Tam, "All-polymer fiber-optic pH sensor," Opt. Express, vol. 26, no. 11, p. 14610, May 2018, doi: 10.1364/oe.26.014610.
[6] X. Yu, D. Bu, X. Chen, J. Zhang, and S. Liu, "Lateral Stress Sensor Based on an In-Fiber Mach–Zehnder Interferometer and Fourier Analysis," IEEE Photonics J., vol. 8, no. 2, pp. 1–10, Apr. 2016.
[7] X. Peng, Y. Cha, H. Zhang, Y. Li, and J. Ye, "Light intensity modulation temperature sensor based on U-shaped bent single-mode fiber," Optik, vol. 130, pp. 813–817, Feb. 2017, doi: 10.1016/j.ijleo.2016.11.003.
[8] J.-M. Hsu, J.-Z. Chen, and W.-H. Zheng, "Highly Sensitive Temperature Fiber Sensor Based on Mach-Zehnder Interferometer," Fiber and Integrated Optics, vol. 35, no. 5–6, pp. 230–238, Aug. 2016, doi: 10.1080/01468030.2016.1214992.
[9] B. Huang, Y. Wang, C. Liao, and Y. Wang, "Highly Sensitive Temperature Sensor Based on All-Fiber Polarization Interference Filter With Vernier Effect," IEEE Access, vol. 8, pp. 207397–207403, 2020.
[10] H. Zhang et al., "Ultrasensitive Mach-Zehnder Interferometric Temperature Sensor Based on Liquid-Filled D-Shaped Fiber Cavity," Sensors, vol. 18, no. 4, p. 1239, Apr. 2018, doi: 10.3390/s18041239.
[11] Y. Zhang, J. Zou, and J.-J. He, "Temperature sensor with enhanced sensitivity based on silicon Mach-Zehnder interferometer with waveguide group index engineering," Opt. Express, vol. 26, no. 20, p. 26057, Sep. 2018.
[12] P. Munendhar, L. Zhang, L. Tong, and S. Yu, "Highly sensitive temperature sensor using intrinsic Mach-Zehnder interferometer formed by bent micro-fiber embedded in polymer," in 25th International Conference on Optical Fiber Sensors, 2017.
[13] L. Ma, Z. Kang, Y. Qi, and S. Jian, "Fiber-optic temperature sensor based on a thinner no-core fiber," Optik, vol. 126, no. 9–10, pp. 1044–1046, May 2015.
[14] K. Tian et al., "High sensitivity temperature sensor based on singlemode-no-core-singlemode fibre structure and alcohol," Sensors and Actuators A: Physical, vol. 284, pp. 28–34, Dec. 2018.
[15]F. Wang, K. Pang, T. Ma, X. Wang, and Y. Liu, "Folded-tapered multimode-no-core fiber sensor for simultaneous measurement of refractive index and temperature," Optics & Laser Technology, vol. 130, p. 106333, Oct. 2020.
[16] X. Lian, Q. Wu, G. Farrell, and Y. Semenova, "High-sensitivity temperature sensor based on anti-resonance in high-index polymer-coated optical fiber interferometers," Opt. Lett., vol. 45, no. 19, p. 5385, Sep. 2020.
[17] C. Li et al., "A Review of Coating Materials Used to Improve the Performance of Optical Fiber Sensors," Sensors, vol. 20, no. 15, p. 4215, Jul. 2020.
[18] Y. Liu and L. B. Yuan, "Ultrasensitive temperature sensor based on a urethane acrylate-coated off-axis spiral long period fiber grating," Optik, vol. 223, p. 165557, Dec. 2020.
[19] Y.-C. Liao et al., "High Temperature (Up to 950 °C) Sensor Based on Micro Taper In-Line Fiber Mach–Zehnder Interferometer," Applied Sciences, vol. 9, no. 12, p. 2394, Jun. 2019.
[20] D. A. May-Arrioja, V. I. Ruiz-Perez, D. Lopez-Cortes, and N. Lozano-Crisostomo, "Linear multimode interference fiber temperature sensor using the liquid in glass thermometer principle," Appl. Opt., vol. 58, no. 14, p. 3856, May 2019.
[21] V. Bhardwaj, R. K. Gangwar, and V. K. Singh, "Silicone rubber-coated highly sensitive optical fiber sensor for temperature measurement," Opt. Eng, vol. 55, no. 12, p. 126107, Dec. 2016.
[22] E. Li and G.-D. Peng, "Wavelength-encoded fiber-optic temperature sensor with ultra-high sensitivity," Optics Communications, vol. 281, no. 23, pp. 5768–5770, Dec. 2008.
[23] M. Kreuzer, "Strain Measurement with Fiber Bragg Grating Sensors." *Ae.metu.edu.tr*, 2006.
[24] D. I. Al-Janabi, A. M. Salman, and A. Al-Janabi, "High-sensitivity balloon-like thermometric sensor based on bent single-mode fiber," Meas. Sci. Technol., vol. 31, no. 11, p. 115106, Sep. 2020.
[25] J. He et al., "High-Sensitivity Temperature Sensor Based on a Coated Single-Mode Fiber Loop," J. Lightwave Technol., vol. 33, no. 19, pp. 4019–4026, Oct. 2015.
[26] T. Zhou, Y. Zhang, B. Han, A. Zhang, and D. Fu, "Low cost non-adiabatic tapered fiber for high-sensitive temperature sensing," Optical Fiber Technology, vol. 45, pp. 53–57, Nov. 2018.

[27] I. Hernandez-Romano, D. Monzon-Hernandez, C. Moreno-Hernandez, D. Moreno-Hernandez, and J. Villatoro, "Highly Sensitive Temperature Sensor Based on a Polymer-Coated Microfiber Interferometer," IEEE Photon. Technol. Lett., vol. 27, no. 24, pp. 2591–2594, Dec. 2015.
[28] P. Wang, H. Zhao, X. Wang, G. Farrell, and G. Brambilla, "A Review of Multimode Interference in Tapered Optical Fibers and Related Applications," Sensors, vol. 18, no. 3, p. 858, Mar. 2018.
[29] L. Hou, X. Zhang, J. Yang, J. Kang, and L. Ran, "Simultaneous measurement of refractive index and temperature based on half-tapered SMS fiber structure with fringe-visibility difference demodulation method," Optics Communications, vol. 433, pp. 252–255, Feb. 2019.
[30] J. Dong, M. Sang, S. Wang, T. Xu, Y. Wang, and T. Liu, "A Novel Mach–Zehnder Interferometric Temperature Sensor Based on a Symmetrical Double-Grooved Structure," IEEE Sensors J., vol. 20, no. 24, pp. 14850–14856, Dec. 2020.
[31] Y. S. Mezaal, S. F. Kareem, "Affine Cipher Cryptanalysis Using Genetic Algorithms," JP Journal of Algebra, Number Theory and Applications, vol. 39, no. 5, pp. 785-802, 2017.
[32] A. Sallomi, S. A. Hashem, and Y. S. Mezaal "A Novel Theoretical Model for Cellular Base Station Radiation Prediction," International journal of simulation: systems, science and technology, vol. 19, no. 6, 2018.
[33] Q. Wang et al., "Optical fiber temperature sensor based on a Mach-Zehnder interferometer with single-mode-thin-core-single-mode fiber structure," Review of Scientific Instruments, vol. 91, no. 1, p. 015006, Jan. 2020.